How to cite: *Angew. Chem. Int. Ed.* **2024**, *63*, e202405636
doi.org/10.1002/anie.202405636

VIP **Photoacoustics** *Very Important Paper*

# Merged Molecular Switches Excel as Optoacoustic Dyes: Azobenzene–Cyanines Are Loud and Photostable NIR Imaging Agents

*Markus Müller, Nian Liu, Vipul Gujrati, Abha Valavalkar, Sean Hartmann, Pia Anzenhofer, Uwe Klemm, András Telek, Benjamin Dietzek-Ivanšić, Achim Hartschuh, Vasilis Ntziachristos, and Oliver Thorn-Seshold**

**Abstract:** Optoacoustic (or photoacoustic) imaging promises micron-resolution noninvasive bioimaging with much deeper penetration (>cm) than fluorescence. However, optoacoustic imaging of enzyme activity would require loud, photostable, NIR-absorbing molecular contrast agents, which remain unknown. Most organic molecular contrast agents are repurposed fluorophores, with severe shortcomings of photoinstability or phototoxicity under optoacoustic imaging, as consequences of their slow $S_1 \rightarrow S_0$ electronic relaxation. We now report that known fluorophores can be rationally modified to reach ultrafast $S_1 \rightarrow S_0$ rates, without much extra molecular complexity, simply by merging them with molecular switches. Here, we merge azobenzene switches with cyanine dyes to give ultrafast relaxation (<10 ps, >100-fold faster). Without even adapting instrument settings, these azohemicyanines display outstanding improvements in signal longevity (>1000-fold increase of photostability) and signal loudness (>3-fold even at time zero). We show why this simple but unexplored design strategy can still offer stronger performance in the future, and can also increase the spatial resolution and the quantitative linearity of photoacoustic response over extended longitudinal imaging. By bringing the world of molecular switches and rotors to bear on problems facing optoacoustic agents, this practical strategy will help to unleash the full potential of optoacoustic imaging in fundamental studies and translational uses.

## *Introduction*

The idea of designing chromophores for ultrafast $S_1 \rightarrow S_0$ electronic relaxation has not yet been raised as a goal for optimising molecular NIR optoacoustic contrast agents, but we feel it will be crucial for successful translation of optoacoustic imaging. Here, we bring it to the community, by showing how a simple design lowers $S_1 \rightarrow S_0$ lifetimes by >100-fold, and thus delivers substantial improvements to currently limited signal strength (here: >7-fold) and dye photostability (>1000-fold).

Optoacoustic imaging, interchangeably called photoacoustics or "PA", adds new opportunities to the imaging toolbox. In PA, short laser pulses excite optical absorbers; when they locally dissipate the excitation energy as heat during the pulse, an expansion pressure wave results, that can be detected with low attenuation and high localisation by ultrasound transducers.[1] With its unique optical-input/acoustic-output combination, PA offers attractive features that other imaging techniques do not: PA penetrates several cm through tissue, with resolution down to 150 μm, and can image endogenous or exogenous contrast agents (by MSOT,

[*] M. Müller, A. Telek, Dr. O. Thorn-Seshold
Department of Pharmacy
LMU Munich
Butenandtstrasse 7, Munich 81377, Germany
E-mail: oliver.thorn-seshold@cup.lmu.de

Dr. N. Liu, Dr. V. Gujrati, P. Anzenhofer, U. Klemm, Prof. Dr. V. Ntziachristos
Institute of Biological and Medical Imaging
Helmholtz Zentrum München
Ingolstaedter Landstrasse 1, Neuherberg 85764, Germany

Dr. N. Liu, Dr. V. Gujrati, Prof. Dr. V. Ntziachristos
Chair of Biological Imaging at the Central Institute for Translational Cancer Research (TranslaTUM)
School of Medicine and Health
Technical University of Munich
Ismaninger Str. 22, Munich 81675, Germany

A. Valavalkar, Prof. Dr. B. Dietzek-Ivanšić
Institute of Physical Chemistry
University of Jena
Lessingstraße 4, Jena 07743, Germany

A. Valavalkar, Prof. Dr. B. Dietzek-Ivanšić
Research Department Functional Interfaces
Leibniz Institute of Photonic Technology Jena
Albert-Einstein-Straße 9, Jena 07745 Germany

S. Hartmann, Prof. Dr. A. Hartschuh
Department of Chemistry
LMU Munich
Butenandtstrasse 8, Munich 81377, Germany



 

multispectral optoacoustic tomography).[2,3] Thus, PA has become valuable particularly in anatomical imaging, from basic research[4] to image-guided surgery.[5]

PA's ultrasound output has excellent tissue penetration; its depth limits come from its optical input. NIR light attenuates the least during tissue penetration,[6] so PA adopted NIR dyes as exogenous contrast agents. Cyanine (Cy) dyes played a major role[7] because of their strong NIR absorption and their rational wavelength tuning capacities, that had been developed for fluorescence.[8] In particular, as the Cy dye indocyanine green (**ICG**; $\lambda_{max} \approx 780$ nm, Figure 1c) is FDA-approved for fluorescence imaging, it was rapidly adopted in PA and is still widely used.[9,10]

Cyanines are still very actively researched: e.g. as SWIR (1–2 μm) fluorophores enabling deeper tissue penetration,[11–13] or as hybrid "hemicyanines"[14] that are easier to make into fluorogenic[15] or acoustogenic[16–18] probes. Other fluorophore and PA contrast agent structural scaffolds have been excellently reviewed.[7,19–22]

However, there has been little rational development of contrast agents to optimise the specific properties needed for PA; in fact, principles for best PA are not even widely agreed upon. Thus, accessible fluorophores, such as Cy dyes, continue to be widely used even though the properties that make them good fluorophores lead to diverse problems when used in PA. These issues have been well-reviewed by Rochford.[23] An optoacoustic signal is proportional to the fraction of absorbed optical energy which is dissipated as heat by vibrational relaxation (**VR**). An obvious drawback of good fluorophores is that they undergo fast VR from hot $S_1$ states to a cold $S_1$ state, but then emit the remaining energy as fluorescence: so overall they convert little energy to optoacoustic signal (Figure 1a).

Yet, most NIR fluorophores are "bad," in the sense that their quantum yields are already low (e.g. 10 %): so further lowering[24–27] or fully quenching[28–30] fluorescence can only increase PA signal by 10 %,[31] unless other mechanisms are also involved.[32] Two such mechanisms for PA enhancement are possible, and were well outlined by Rochford.[23] In brief, since PA supplies energy during infrequent excitation pulses that have similar duration as typical $S_1$ state lifetimes (pulses ~ns, ~10 Hz repeat rate), time-dependent effects become important:

(**1**) If relatively long-lived $S_1$ states can be excited further to $S_n$ states during a PA pulse, these typically vibrationally relax rapidly back to $S_1$. In theory, fast $S_1 \rightarrow S_n \rightarrow S_1$ cycling such "**RSA**" chromophores (reverse-saturable absorbers) can thus allow higher PA signal than ordinary chromophores using $S_0 \rightarrow S_1 \rightarrow S_0$ cycles ("**SA**", saturable absorbers), since $S_n \rightarrow S_1$ is faster than $S_1 \rightarrow S_0$. RSAs have been widely reported in cell-free PA studies.[23] However, RSA signal scales non-linearly with laser fluence, since the signal comes from doubly excited species ($S_0 \rightarrow S_1$ then $S_1 \rightarrow S_n$). Biologically allowed energy limits dictate such low fluence in deep tissue that in practice, RSAs are outperformed by ordinary PA emitters that simply absorb light more strongly.[33,34] We also argue that cycling RSAs between $S_1/S_n$ states may cause photoreactive damage to the chromophore or to biological tissues.

(**2**) Alternatively, if $S_1$ becomes very short-lived (lifetime ≪ laser pulse length), in theory multiple $S_0 \rightarrow S_1 \rightarrow S_0$ excitation/VR cycles will be possible in a single pulse, also increasing the optoacoustic signal compared to ordinary chromophores (Figure 1b). Rochford named these "**LA**" chromophores (linear absorbers), since their PA signal should scale linearly to the excitation intensity, though only one was identified: the genotoxic 580 nm-absorbing dye crystal violet.[23,35] We argue that if molecular NIR LAs can be made, they hold the

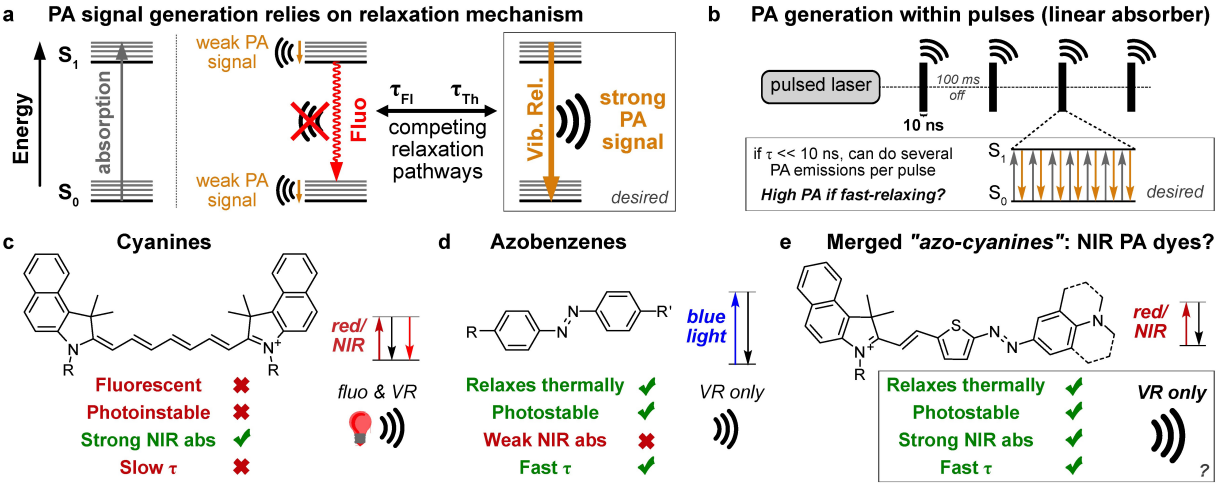


***Figure 1.*** Design concept for molecular switch-based optoacoustic contrast agents. a) Energy dissipated as heat contributes to PA signal (internal conversion then vibrational relaxation); fluorescence does not. b) PA excitation is pulsed. For a linear absorber ($S_1 \rightarrow S_0$ relaxation halflife τ much shorter than the pulse), several $S_0 \rightarrow S_1 \rightarrow S_0$ excitation-relaxation cycles are possible within one pulse. c) Cyanine dyes have strong NIR absorption, but are poor PA agents as they are slow-relaxing and non-photostable. d) Azobenzenes have ultrafast nonradiative relaxation, but as UV/Vis-absorbers they are not useful for NIR PA. e) **Hypothesis**: merging azobenzenes and cyanines should give strong, photostable NIR-absorbing PA emitters.

key to successful molecular PA, for two reasons that we did not yet find discussed together:

(**2a**) Photoinstability is a major drawback for NIR fluorophores currently used in PA. A typical case is **ICG** which bleaches out in minutes (Figure 3d).[36,37] This not only limits the imaging time-window, but makes a signal not quantitative for probe concentration, but only for its non-photobleached fraction. Instead, LAs should be very photostable, since rapid depletion of $S_1$ prevents excited-state photoreactivity: thus LAs should allow long-term/longitudinal imaging, with accurate signal quantification, as is needed for molecular PA imaging.[38]

(**2b**) LAs should give a predictable, useful response in biology, since they suffer only proportional signal decrease as the excitation power attenuates with depth (contrast this to nonlinear response of RSAs).

We recognised that molecular switches such as azobenzenes, which $S_1 \rightarrow S_0$ relax with picosecond halftimes and which, accordingly, have been exploited as enormously photostable dyes since >170 years,[39,40] would be an ideal LA chemotype; and that this parallels Rochford's recognition of crystal violet (a molecular rotor) as an excellent LA. There were encouraging hints that *appropriate* azobenzenes could succeed in PA. The non-emissivity and photostability of azobenzenes makes them popular as fluorescence quenchers in FRET probes, if excitation energy can be transferred onto them;[41] and in Gambhir's early work on acoustogenic probes, the complex azobenzene **BHQ3** was by chance found to be an "unusually strong" PA emitter, although the reasons for this were not explored and the work was not pursued further.[32] However, we knew of no biocompatible / water-soluble azobenzenes absorbing suitably in the ideal NIR window for PA (760–880 nm)[42] that could be tested (Figure 1d).

We now show the feasibility of rationally creating LA-type, NIR-absorbing, highly photostable and loud PA chromophores allowing multiple excitations per pulse, by uniting good chromophores and good switches. Our proof of principle work unites the NIR absorption of Cy dyes (strong chance to enter $S_1$) with the relaxation of azobenzene-type molecular switches (for ultrafast $S_1 \rightarrow S_0$; Figure 1e).

## Results and Discussion

### Design, Synthesis, and Spectral Properties

Our first approach was to attach the phenylazo switch onto Cy5/7 fluorophores, at the middle (**M-AzCy5**) or the end (**E-AzCy5/7**; Figure 2). In the second approach, we replaced part of the π-system with the azobenzene, imagining that conjugating over its N=N would maximise relaxation rates. This gave azo-hemicyanines, with phenylazobenzene systems of two π-system lengths (**P-AzHCy1/2**). Like Nakamura, who used thiophenylazo bridges for redshifting,[43] we also tested thiophenylazos with two donor group types (**T-AzHCy1/2**). Interestingly, Swager had suggested to use such scaffolds for PA imaging,[44] but the lack of water solubility had presumably blocked it. To force water solubility, we also installed an extra sulfonate in **wsT-AzHCy** (Figure 2).

Their syntheses were direct. The middle phenylazo was installed by reacting the pentamethine with phenyldiazo-

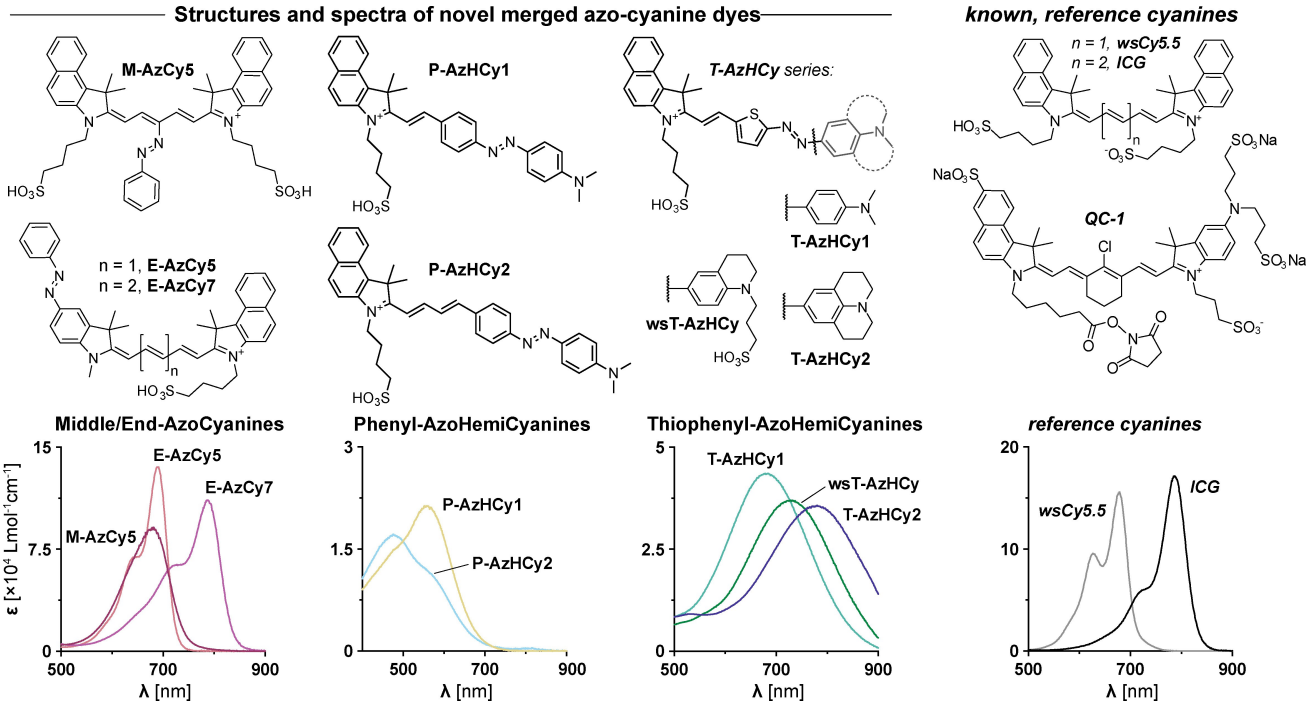


***Figure 2.*** Structures and absorption spectra of azo-cyanines (dyes in 1:1 EtOH:PBS at 10 μM, except **ICG** at 5 μM; further details in Figure S1).

nium (**M-AzCy5**);[45] the end phenylazos were installed onto the indolenin before the polymethines were synthesised by asymmetric Cy dye syntheses (**E-AzCy5/7**; Scheme S1). The azo-hemicyanines were synthesised by Knoevenagel condensation of the indolene and the aldehydes (**P/T-AzHCy1/2**, **wsT-AzHCy**; Scheme S2).

The first requirement for these dyes was to reach strong NIR absorption, with $\lambda_{max}$ desired as >720 nm for in vivo applicability. Middle/end azo-cyanine **M/E-AzCy**s had similar absorption as the reference pentamethine **wsCy5.5** or heptamethine **ICG**, though were broadened and at lower intensity, as expected.[46,47] The phenylazo-hemicyanine **P-AzHCy** types absorb in the cyan/green, so were not continued for further study. Pleasingly, the thiophenylazo-hemicyanine **T-AzHCy** types had strong absorption in the PA-adapted NIR window, with the $\lambda_{max}$ value of 779 nm for **T-AzHCy2** being directly comparable to **ICG**; though again, their bands were broader and had lower extinction coefficients than the symmetric Cy dyes (Figure 2, Table 1).

The next requirement was to reach LA-type PA agents, by forcing an ultrashort-lived $S_1$ state. Low fluorescence is a necessary but insufficient proof of short $S_1$ lifetime. The **T-AzHCy** types had zero detectable fluorescence on our usual setup; **M-AzCy5** was almost nonfluorescent, but $\Phi_{FL}$ of **E-AzCy5/7** barely differed from their parents (Table 1; we return to the $S_1$ lifetimes later, at Table 2).

Azobenzenes can undergo E⇄Z photoisomerizations[48] that change their absorption profiles. For quantifying a PA contrast agent, such changes would be an undesirable. We tested the **T-AzHCy** types that were now our leads, and these did not change Vis/NIR absorption under strong LED illumination, which is promising but not yet conclusive (discussion at Figure S2, see also TA spectroscopy below).

### *Strength and Photostability of the Optoacoustic Signal*

We now tested our hypothesis that azo-merged-cyanines with fast $S_1 \rightarrow S_0$ VR would have strong, photostable, optoacoustic signals.

We first determined PA response spectra. Pleasingly, the **T-AzHCy**s and **M-AzCy** gave much stronger PA than **ICG** across broad spectral ranges, despite all being tested at the same optical density: an indication that they function as LAs, not SAs (Figure 3a). For an ideal and quantitative LA, the photoacoustic response spectrum should match the absorption spectrum: and indeed, they had perfect spectral overlay, which suits them as scaffolds for strong, linear, quantitative PA imaging over a range of wavelengths (Figure S3; a counterexample is provided by SA **ICG**, whose spectra differ strongly; contributing to its PA response being nonlinear and environment-dependent).[50]

To quantify the PA signal generation efficacy (SGE) robustly, we determined the PA-to-OD fits across the full OD range 0.1–0.5, which were linear for all species (Figure S4; comparison to cyanine-type reference compounds **wsCy5.5** and **QC-1** in Figures S5 and S6). Pleasingly, **wsT-AzHCy** and **T-AzHCy2** were excellently strong PA emitters, with SGE >3 times that of **ICG**. **M-AzCy5** was also a very strong PA emitter; **E-AzCy5/7** had the lowest SGE, similar to **ICG** (Figure 3b). Noteworthily, these PA signal enhancements up to +220 % (Figure 3b) far surpass the +10 % expected for pure fluorescence quenching: supporting the hypothesis of multiple excitations per pulse, which is expected to be a *fully general* advantage of the merged switch approach. (As a corollary of this: although the quantum yield $\Phi_{nr}$ for non-radiative decay following a single excitation is the typical way of rationalising photoacoustic efficiency, we can state that the enhanced photoacoustic signal does *not* directly arise from an increase in $\Phi_{nr}$ but rather is a time-dependent effect since multiple excitations are possible in a row).

***Table 1:*** Absorption (1 : 1 EtOH:PBS) and fluorescence (EtOH).

| | $\lambda_{max}$ [nm] | ε [×10³ $M^{-1}cm^{-1}$] | FWHM [nm] | $\Phi_{FL}$ |
|---|---|---|---|---|
| **M-AzCy5** | 678 | 94 | 100 | <0.01 |
| **E-AzCy5** | 689 | 136 | 72 | 0.22 |
| **E-AzCy7** | 785 | 111 | 114 | 0.10 |
| **P-AzHCy1** | 557 | 48 | 162 | *not tested* |
| **P-AzHCy2** | 483 | 28 | 245 | *not tested* |
| **T-AzHCy1** | 685 | 44 | 189 | $<10^{-3}$ |
| **T-AzHCy2** | 779 | 35 | 220 | $<10^{-3}$ |
| **wsT-AzHCy** | 729 | 37 | 199 | $<10^{-3}$ |
| ***wsCy5.5*** | *679* | *156* | *82* | *0.31* |
| ***ICG*** | *787* | *172* | *56* | *0.13 (lit.[49])* |

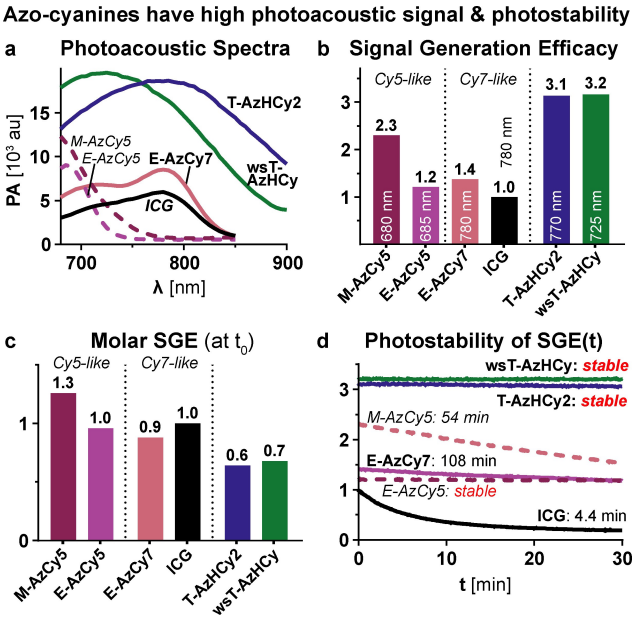


***Figure 3.*** Optoacoustic properties in 1 : 1 PBS:EtOH. a) Photoacoustic spectra. b) PA signal generation efficacy (SGE) at constant OD, showing relative dye "loudness". c) SGE adjusted to constant molarity (**ICG** set to 1). d) PA photostability determination. (a,d: measured at OD = 0.5 at $\lambda_{max}$ [values given in panel b]; excitation in d performed at $\lambda_{max}$).

The photoacoustic performance enhancement for **AzHCy** over **ICG** is even greater when measured under more physiological conditions, i.e. with serum and without organic cosolvent: with SGE of **wsT-AzHCy** being >7 times that of **ICG** (Figure S7).

These *specific* azo-cyanines are band-broadened compared to symmetric cyanines; so if their SGEs are normalised by molarity, their lower extinction coefficients make their *starting* molar PA signal around 1–2 fold of that for the cyanines (Figure 3c, Figure S7). However, it is not the signal before imaging, but signal over time, that is the real challenge. Only PA agents that can be imaged *continually* and accumulate high photon count without bleaching can be useful molecular probes in vivo: otherwise, their signal is not quantitative, but bleaching unpredictably masks the true product concentration.[7] Hoping that the ultrafast relaxation of the merged switches offers a *fully general* solution for stability enhancement, we now measured PA signal profiles over longer times, with typical settings for in vivo imaging (Figure 3d; i.e. laser pulses at 10 mJ/cm$^2$, 10 ns pulsewidth, 10 Hz repetition rate; in vivo image acquisition can take seconds to minutes per section at these settings). The results support our LA design principle excellently. For example, while the PA signal half-life ($t_{1/2}$) of **ICG** is only 4 min under these conditions, the **AzHCy**s simply do not bleach (Figure 3d). Only by using the standard error of their PA signal over 30 minutes as a gross overestimate, could we even estimate a lowest possible bound for their bleaching half-life: with **wsT-AzHCy** as >140 hours, i.e. >1900 times more stable than **ICG**; isoelectronic **T-AzHCy2** was similar (Supporting Information 3.3). The mid-/end-attached **M-AzCy5/E-AzCy5/7** were also >10-fold more photostable than their cyanine congeners. The excellent **AzHCy** photostability is preserved with serum (discussion at Figure S7).

This direct access to **AzHCy** PA dyes that maintain a louder signal intensity for orders of magnitude longer than typical dyes, is the key value of our design: since it allows quantitative rather than only qualitative interpretation of signal intensity, throughout biologically relevant assay timescales. Even focusing just on crude signal, the 3–7-fold higher SGE of **AzHCy**s plus their *total* resistance to photobleaching let them surpass the higher extinction coefficients of photobleachable **ICG** to deliver far higher molar PA signal within a few minutes of imaging (i.e. a few frames, or less). We believe these photostability and SGE enhancements will be generally applicable in other dye/switch families too, enabling current dyes to withstand higher pulse energies in long-term imaging while also maintaining higher signal intensity: which is crucial for imaging low-turnover enzyme activity, by accumulating quantitative and stable signal over time.

### *Excited State Lifetimes and Evolution*

The loud and photostable contrast agents we anticipated in these designs (Figure 1e) had been validated experimentally. Next, to see if the mechanisms we had anticipated were responsible for this performance, we tested if the excited state lifetimes for the new PA contrast agents had been shortened far below the laser pulse length: needed to allow the several excitations per pulse that the SGE data suggested. First, we used time-resolved fluorescence spectroscopy[51] on a high-sensitivity setup, to capture the weak AzHCy fluorescence (spectra in Figure S9). The time-resolved fluorescence data were used to extract $S_1$ decay time constants (Figure 4a). Matching our hopes, the most photostable compounds **T-AzHCy2** and **wsT-AzHCy** relaxed electronically with ultrafast time constants $\tau_{PL}$ of just approximately10 ps: which is $10^3$-fold shorter than the PA laser pulse duration (10 ns). **M-AzCy5** and **E-AzCy5/7** had much longer time constants, ca. 540 and 370 ps respectively. This trend matches the involvement of the diazene in the π-system (**T-AzHCy**: integral; **E/M-AzCy**: attached).

For multiple $S_0 \rightarrow S_1 \rightarrow S_0$ excitation/emission cycles per pulse, the depopulation of $S_1$ must be fast, as the luminescence data confirm, but the ground state must also be reached without other significant photoproducts.[23,33] Therefore, we next used transient absorption (TA) spectroscopy to study the excited state evolution. Pleasingly, both **T-AzHCy**s returned to the groundstate with ultrafast kinetics by a simple monoexponential $S_1 \rightarrow S_0$ path ($\tau_{TAS} \approx 4$ ps; the slower species **M-AzCy5** takes a biexponential path with overall halftime ca. 100 ps; Figure 4b–d, Figure S10). Although acquired in different solvents, the TA and luminescence lifetimes match. Thus, our "star" species show the set of properties we had targeted for loud, linear PA emitters (Table 2): ultrafast excited state decay to the groundstate allowing multiple $S_0 \rightarrow S_1 \rightarrow S_0$ cycles per pulse, associated to outstanding photostability and excellent SGE, just as desired for easy and reliable quantification in NIR optoacoustic imaging.

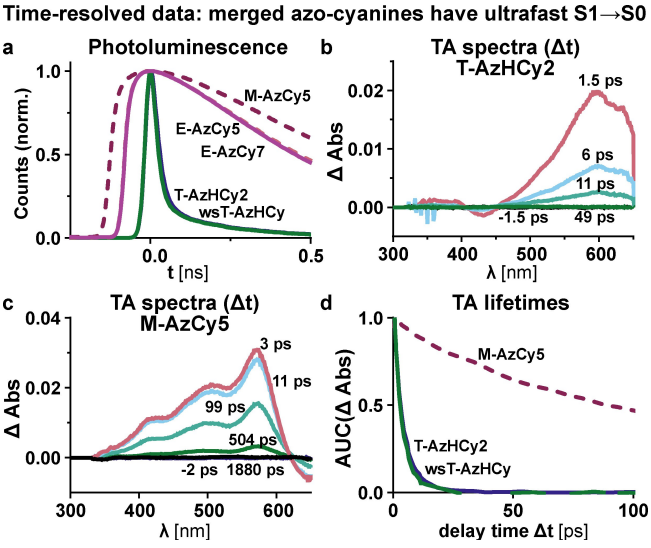


***Figure 4.*** Time-resolved data. a) Fluorescence shows decay rates of singlet excited states. b–d) Transient absorption (TA) spectroscopy: **T-AzHCy2** relaxes fully to $S_0$ with $\tau_{TAS} \approx 4$ps, but **M-AzCy5** has $\tau_{TAS} \approx 180$ ps. d) TA ΔAbs decays (fitted lifetimes given in Table 2).

*Table 2:* Summary of key optoacoustic parameters.

| | Photoacoustic response | | | Elec. relaxation | |
|---|---|---|---|---|---|
| | $\lambda_{SGE}$ [nm] | Signal (SGE) | stability $t_{1/2}$ [min] | $\tau_{PL}$[a] [ps] | $\tau_{TAS}$ [ps] |
| **M-AzCy5** | 680 | 2.3 | 54 | 540[b] | 180[b] |
| **E-AzCy5** | 685 | 1.2 | ≫4270[c] | 386[b] | *not m.* |
| **E-AzCy7** | 785 | 1.4 | 108 | 363 | *not m.* |
| **T-AzHCy2** | 770 | 3.1 | ≫1400[c] | 13 | 4.0 |
| **wsT-AzHCy** | 740 | 3.2 | ≫8400[c] | 9 | 3.6 |
| ***ICG** (ref.)* | *780* | *1* | *4.4* | *10*[3; d] | *not m.* |

[a] Major decay. [b] Complex fit. [c] Lower bounds. [d] Value from ref. [49]. "*not m.*": not measured.

### *In Vivo Imaging*

The major goal of photoacoustics is to enable in vivo experiments. While the focus of this paper was to put forward a novel chemical concept that we believe can improve photoacoustic performance for many dye classes, we also wished to apply a specific example dye in vivo (choice: **wsT-AzHCy**), for a test of concept of whether ultrafast relaxation delivers real-world usability and utility in PA.

Our goals were to assess important conceptual features that should also be shared with other dyes developed along the azo-merged design: i) if the broad absorption of **wsT-AzHCy** still allows unmixing its signal from that of endogenous chromophores, during standard multispectral optoacoustic tomography (MSOT); ii) if the diazene-containing dye survives in vivo biochemistry/ADME long enough to allow practical use (we chose 120 min), since long survival is a necessary precondition to exploit its longterm photostability; iii) if such designs have promise for adaptation to molecular imaging agents, rather than being restricted to being *anatomical* stains. For example, if the dye is permanently bound to serum albumin, its signal will only map the bloodstream, making it an anatomical imaging agent; but if it non-uniformly distributes between organs, this offers hope that there are significant molecular interactions which may later be tuned by derivatisation e.g. for enzyme-responsive imaging.

In vivo MSOT imaging was thus performed before, and then 2 h after, intravenous (IV) injection of **wsT-AzHCy** into the lateral tail vein of healthy adult mice. Transverse image sections were chosen to visualize the organs where molecular dyes are typically accumulated: liver (Figure 5a,b), kidney and spleen (Figure 5c,d).

(**i,ii**) Spectral unmixing quantified strong specific **wsT-AzHCy** signal 2 h post injection, without significant background before injection. MSOT can therefore successfully separate the dye from endogenous background, and the azo-merged dye has a good survival time in vivo (Figure 5).

(**iii**) The **wsT-AzHCy** signal had a clear biodistribution to the gut, spleen, and liver, but exclusion from the kidneys (Figure 5b,d). This is a promising indication of molecular accessibility, that it may be possible to harness later for molecular imaging.

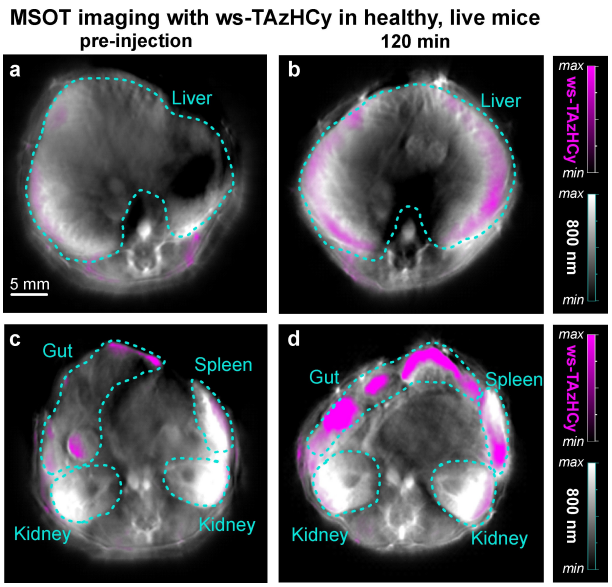


***Figure 5.*** In vivo MSOT images. Transverse image sections of live, healthy mice, showing a,b) liver, c,d) kidney and spleen, each before and 120 min after IV injection of **wsT-AzHCy** (100 µL, 0.5 mM) under the same image acquisition conditions. Imager: MSOT inVision 256-TF (iThera, Germany; 800 nm image is the anatomical imaging reference frame (essentially, blood content); **wsT-AzHCy** image is calculated by spectral deconvolution).[52]

Taken together, this proof-of-concept experiment gave promising indications for the usability of photoacoustic contrast agents based on merged molecular switches in live animal imaging.

## *Conclusion*

The great advances in biology have in large part been driven by chemical chromophores. Fluorophores, which easily enable quantitative imaging of live cell enzymatic activity, have for several decades been tuned e.g. for shallow in vivo imaging.[53] The equipment and engineering necessary to instead harness the optoacoustic response of chromophores for deep in vivo imaging is now becoming available. Yet, to realise its promise for quantitative imaging in live animal as well as clinical settings, we must move beyond repurposing poorly adapted contrast agents such as fluorophores: we must rationally develop chemical design strategies for optoacoustic chromophores, tailored to the unique challenges and opportunities of PA.

Here, we have focused on the $S_1 \rightarrow S_0$ lifetime: one of the most powerful photophysical regulators of PA contrast agent performance, but which has been chemically almost ignored.

We showed that the rational integration of molecular switches into NIR-absorbing scaffolds can accelerate their $S_1 \rightarrow S_0$ transition by >100-fold. This gives a >1000-fold enhancement of PA signal photostability, while also convert-

ing even poorly quantifiable "saturable absorber" chromophores into "linear absorber" PA contrast agents that promise to be reliably and stably quantifiable at arbitrary illumination intensity, over arbitrarily long imaging timecourses. By permitting many $S_0 \rightarrow S_1 \rightarrow S_0$ cycles per pulse, **AzHCy** offer a simple organic chromophore method to multiply PA signal response: and even on current standard PA equipment, with relatively long pulse settings that are optimised around the weaknesses of current SAs, these ultrafast-relaxing **AzHCy** agents already provide 3–7 fold higher signal generation efficacy at the start of imaging. However, their linear response to excitation intensity offers an opportunity to harness shorter but more intense excitation pulses to deliver the same or higher PA signal intensity output, but with higher resolution and lower background, which no current NIR-active organic PA contrast agents can provide (since fast relaxation is needed to harness short pulses; Figure S12).

Conceptually, when we began this work, we did not locate an accessible analytical framework that would convincingly predict to colleagues how the multiple performance features that must *all* be balanced for high-performance PA, should all be improved to varying degrees by accelerating non-radiative $S_1 \rightarrow S_0$ decay: i.e. (1) photostability and (2) signal loudness in arbitrary settings, as we report here; but also, e.g., (3) signal loudness and (4) signal-to-background ratio and (5) excitation voxel resolution, each as a function of excitation pulse timing and intensity (Figure S12). During paper revisions, we were delighted that Brøndsted and Stains posted a preprint[31] parametrising an Acoustic Loudness Factor ($ALF = k_{nr} \times \varepsilon$) that, as we do, now *explicitly* prioritises non-radiative decay rates in which linear absorbers excel to guide PA dye optimisation (ALF corresponds to point 2, loudness in arbitrary settings, in our treatment). Since it is straightforward to determine ALF reliably even without PA equipment, we believe ALF will prove more useful than previous parametrisations that apply only to saturable absorbers and have oriented research into dead ends,[31] even though ALF does not report other relevant aspects like photostability, ISC, and pulse-dependency effects.

Practically, since this rational merged-switch design hypothesis succeeded so directly, we predict that remastering molecular switches will become a powerful route to enhance the photophysically determined performance features of chromophores in a truly general sense. For example, the broadened NIR absorption of the nonfluorescent **AzHCy**s (beyond 900 nm for **T-AzHCy2**, and easily tunable) makes them ideal candidate NIR fluorescence quenchers (another molecularly underrepresented class of imaging agent) e.g. for off→ON, NIR, FRET probes. PA also faces other challenges for engineering the photophysics and biocompatibility of its chromophores,[23] but we believe that they too can be solved in a modular way that can synergise with the benefits of ultrafast relaxation. Perhaps the most significant of these, is to introduce enzyme-responsive[54,55] molecular PA imaging for the NIR/SWIR region.[56,57] In this respect, Schnermann's enzyme-activatable NIR cyanine template (CyBam)[58] may offer an ideal model system to synergise with the arylazo-cyanines developed here. We are convinced that the scope for other chromophore types, as well as other chemotypes of switches, or rotors and motors, will be broad enough to power much creative harmony: in optoacoustics and beyond.

## Supporting Information

Synthesis, photophysics data, and NMR spectra (PDF). The authors have cited additional references within the Supporting Information.[59–75]

## Abbreviations

| | |
|---|---|
| ADME | absorption, distribution, metabolism and excretion |
| ALF | acoustic loudness factor |
| FRET | fluorescence resonance energy transfer |
| IC | internal conversion |
| ISC | intersystem crossing |
| LA | linear absorber |
| MSOT | multispectral optoacoustic (or photoacoustic) tomography |
| NIR | near-infrared |
| PA | photoacoustic (or optoacoustic) signal generation or imaging |
| RSA | reverse-saturable absorber |
| SA | saturable absorber |
| SGE | signal generation efficiency |
| SWIR | short-wave infrared |
| VR | vibrational relaxation |

## Acknowledgements

This research was supported by funds from the Boehringer Ingelheim Stiftung (Exploration Grant to O.T.-S.) and the German Research Foundation (DFG: Emmy Noether grant number 400324123 to O.T.-S.; SFB 1032 number 201269156 project B09 to O.T.-S.; SFB TRR 152 number 239283807 project P24 to O.T.-S.; SPP 1926 number 426018126 project XVIII to O.T.-S.; CRC 1123 (Z1) to V.N.; SFB 1278 PolyTarget, project A03 to B.D.-I.). We thank Jan Felber (LMU) for assistance in PA imaging; Michaela Kaltenegger and Jan Philip Prohaska (LMU) for synthetic support and cordial discussions; Viktorija Glembockyte (LMU) for mechanistic discussions and advice on photophysical applications; and Eberhard Riedle (LMU) for motivation and discussions around using transient absorption spectroscopy for mechanistic studies. We acknowledge support from the Joachim Herz Foundation (Research Fellowship to M.M.). Open Access funding enabled and organized by Projekt DEAL.

## Conflict of Interest

V.N. is a founder and equity owner of sThesis GmbH, iThera Medical GmbH, Spear UG and I3 Inc.

## Data Availability Statement

The data that support the findings of this study are available in the Supporting Information, and related data are available from the corresponding author upon reasonable request.

**Keywords:** optoacoustic imaging · photoacoustic dyes · photoswitches · fluorescence · quenchers

[1] V. Ntziachristos, *Nat. Methods* **2010**, *7*, 603–614.
[2] V. Ntziachristos, D. Razansky, *Chem. Rev.* **2010**, *110*, 2783–2794.
[3] A. Taruttis, V. Ntziachristos, *Nat. Photonics* **2015**, *9*, 219–227.
[4] A. Karlas, M. A. Pleitez, J. Aguirre, V. Ntziachristos, *Nat. Rev. Endocrinol.* **2021**, *17*, 323–335.
[5] C. Moore, J. V. Jokerst, *Theranostics* **2019**, *9*, 1550–1571.
[6] S. L. Jacques, *Phys. Med. Biol.* **2013**, *58*, R37–R61.
[7] V. Gujrati, A. Mishra, V. Ntziachristos, *Chem. Commun.* **2017**, *53*, 4653–4672.
[8] A. P. Gorka, R. R. Nani, M. J. Schnermann, *Acc. Chem. Res.* **2018**, *51*, 3226–3235.
[9] N. Beziere, N. Lozano, A. Nunes, J. Salichs, D. Queiros, K. Kostarelos, V. Ntziachristos, *Biomaterials* **2015**, *37*, 415–424.
[10] J. Zhong, S. Yang, X. Zheng, T. Zhou, D. Xing, *Nanomedicine* **2013**, *8*, 903–919.
[11] E. D. Cosco, J. R. Caram, O. T. Bruns, D. Franke, R. A. Day, E. P. Farr, M. G. Bawendi, E. M. Sletten, *Angew. Chem. Int. Ed.* **2017**, *56*, 13126–13129.
[12] E. D. Cosco, A. L. Spearman, S. Ramakrishnan, J. G. P. Lingg, M. Saccomano, M. Pengshung, B. A. Arús, K. C. Y. Wong, S. Glasl, V. Ntziachristos, M. Warmer, R. R. McLaughlin, O. T. Bruns, E. M. Sletten, *Nat. Chem.* **2020**, *12*, 1123–1130.
[13] V. G. Bandi, M. P. Luciano, M. Saccomano, N. L. Patel, T. S. Bischof, J. G. P. Lingg, P. T. Tsrunchev, M. N. Nix, B. Ruehle, C. Sanders, L. Riffle, C. M. Robinson, S. Difilippantonio, J. D. Kalen, U. Resch-Genger, J. Ivanic, O. T. Bruns, M. J. Schnermann, *Nat. Methods* **2022**, *19*, 353–358.
[14] L. Yuan, W. Lin, Y. Yang, H. Chen, *J. Am. Chem. Soc.* **2012**, *134*, 1200–1211.
[15] H. Li, H. Kim, F. Xu, J. Han, Q. Yao, J. Wang, K. Pu, X. Peng, J. Yoon, *Chem. Soc. Rev.* **2022**, *51*, 1795–1835.
[16] M. Y. Lucero, J. Chan, *Nat. Chem.* **2021**, *13*, 1248–1256.
[17] S. H. Gardner, C. J. Brady, C. Keeton, A. K. Yadav, S. C. Mallojjala, M. Y. Lucero, S. Su, Z. Yu, J. S. Hirschi, L. M. Mirica, J. Chan, *Angew. Chem. Int. Ed.* **2021**, *60*, 18860–18866.
[18] S. Zhang, H. Chen, L. Wang, X. Qin, B.-P. Jiang, S.-C. Ji, X.-C. Shen, H. Liang, *Angew. Chem. Int. Ed.* **2021**, *61*, e202107076.
[19] J. Weber, P. C. Beard, S. E. Bohndiek, *Nat. Methods* **2016**, *13*, 639–650.
[20] X. Zhang, Y. Wu, L. Chen, J. Song, H. Yang, *Chem. Biomed. Imaging* **2023**, *1*, 99–109.
[21] Z. Zhao, C. Chen, W. Wu, F. Wang, L. Du, X. Zhang, Y. Xiong, X. He, Y. Cai, R. T. K. Kwok, J. W. Y. Lam, X. Gao, P. Sun, D. L. Phillips, D. Ding, B. Z. Tang, *Nat. Commun.* **2019**, *10*, 768.
[22] C. Xu, R. Ye, H. Shen, J. W. Y. Lam, Z. Zhao, B. Z. Tang, *Angew. Chem. Int. Ed.* **2022**, *61*, e202204604.
[23] M. Hatamimoslehabadi, S. Bellinger, J. La, E. Ahmad, M. Frenette, C. Yelleswarapu, J. Rochford, *J. Phys. Chem. C* **2017**, *121*, 24168–24178.
[24] C. S. L. Rathnamalala, N. W. Pino, B. S. Herring, M. Hooper, S. R. Gwaltney, J. Chan, C. N. Scott, *Org. Lett.* **2021**, *23*, 7640–7644.
[25] N. Liu, V. Gujrati, J. Malekzadeh-Najafabadi, J. P. F. Werner, U. Klemm, L. Tang, Z. Chen, J. Prakash, Y. Huang, A. Stiel, G. Mettenleiter, M. Aichler, A. Blutke, A. Walch, K. Kleigrewe, D. Razansky, M. Sattler, V. Ntziachristos, *Photoacoustics* **2021**, *22*, 100263.
[26] N. Liu, P. O'Connor, V. Gujrati, D. Gorpas, S. Glasl, A. Blutke, A. Walch, K. Kleigrewe, M. Sattler, O. Plettenburg, V. Ntziachristos, *Adv. Healthcare Mater.* **2021**, *10*, 2002115.
[27] X. Zhou, Y. Fang, V. Wimalasiri, C. I. Stains, E. W. Miller, *Chem. Commun.* **2022**, *58*, 11941–11944.
[28] T. Ikeno, K. Hanaoka, S. Iwaki, T. Myochin, Y. Murayama, H. Ohde, T. Komatsu, T. Ueno, T. Nagano, Y. Urano, *Anal. Chem.* **2019**, *91*, 9086–9092.
[29] J. M. Merkes, T. Lammers, R. Kancherla, M. Rueping, F. Kiessling, S. Banala, *Adv. Opt. Mater.* **2020**, *8*, 1902115.
[30] M. Laramie, M. Smith, F. Marmarchi, L. McNally, M. Henary, *Molecules* **2018**, *23*, 2766.
[31] F. Brøndsted, H. Shield, J. Moore, X. Zhou, Y. Fang, C. Stains, *ChemRxiv.* **2024**, DOI 10.26434/chemrxiv-2024-7cbk2.
[32] J. Levi, S. R. Kothapalli, T.-J. Ma, K. Hartman, B. T. Khuri-Yakub, S. S. Gambhir, *J. Am. Chem. Soc.* **2010**, *132*, 11264–11269.
[33] M. Frenette, M. Hatamimoslehabadi, S. Bellinger-Buckley, S. Laoui, J. La, S. Bag, S. Mallidi, T. Hasan, B. Bouma, C. Yelleswarapu, J. Rochford, *J. Am. Chem. Soc.* **2014**, *136*, 15853–15856.
[34] R. E. Borg, M. Hatamimoslehabadi, S. Bellinger, J. La, F. Mithila, C. Yelleswarapu, J. Rochford, *Photochem. Photobiol.* **2019**, *95*, 280–292.
[35] R. E. Borg, J. Rochford, *Photochem. Photobiol.* **2018**, *94*, 1175–1209.
[36] S. S. Matikonda, D. A. Helmerich, M. Meub, G. Beliu, P. Kollmannsberger, A. Greer, M. Sauer, M. J. Schnermann, *ACS Cent. Sci.* **2021**, *7*, 1144–1155.
[37] R. R. Nani, J. A. Kelley, J. Ivanic, M. J. Schnermann, *Chem. Sci.* **2015**, *6*, 6556–6563.
[38] E. M. S. Stennett, M. A. Ciuba, M. Levitus, *Chem. Soc. Rev.* **2014**, *43*, 1057–1075.
[39] H. M. D. Bandara, S. C. Burdette, *Chem. Soc. Rev.* **2012**, *41*, 1809–1825.
[40] J. Garcia-Amorós, B. Maerz, M. Reig, A. Cuadrado, L. Blancafort, E. Samoylova, D. Velasco, *Chem. Eur. J.* **2019**, *25*, 7726–7732.
[41] A. Chevalier, C. Massif, P.-Y. Renard, A. Romieu, *Chem. Eur. J.* **2013**, *19*, 1686–1699.
[42] M. Dong, A. Babalhavaeji, S. Samanta, A. A. Beharry, G. A. Woolley, *Acc. Chem. Res.* **2015**, *48*, 2662–2670.
[43] S. Fuse, T. Oishi, K. Matsumura, Y. Hayashi, S. Kawauchi, H. Nakamura, *Org. Biomol. Chem.* **2019**, *18*, 93–101.
[44] T. M. Swager, L. Delage-Laurin, *Synfacts* **2020**, *16*, 0152.
[45] A. Treibs, R. Zimmer-Galler, *Justus Liebigs Ann. Chem.* **1959**, *627*, 166–181.
[46] L. M. Tolbert, X. Zhao, *J. Am. Chem. Soc.* **1997**, *119*, 3253–3258.
[47] S. Pascal, A. Haefele, C. Monnereau, A. Charaf-Eddin, D. Jacquemin, B. Le Guennic, C. Andraud, O. Maury, *J. Phys. Chem. A* **2014**, *118*, 4038–4047.
[48] G. S. Hartley, *Nature* **1937**, *140*, 281–281.
[49] M. Y. Berezin, S. Achilefu, *Chem. Rev.* **2010**, *110*, 2641–2684.
[50] J. P. Fuenzalida Werner, Y. Huang, K. Mishra, R. Janowski, P. Vetschera, C. Heichler, A. Chmyrov, C. Neufert, D. Niessing,

V. Ntziachristos, A. C. Stiel, *Anal. Chem.* **2020**, *92*, 10717–10724.
[51] M. L. DiFrancesco, F. Lodola, E. Colombo, L. Maragliano, M. Bramini, G. M. Paternò, P. Baldelli, M. D. Serra, L. Lunelli, M. Marchioretto, G. Grasselli, S. Cimò, L. Colella, D. Fazzi, F. Ortica, V. Vurro, C. G. Eleftheriou, D. Shmal, J. F. Maya-Vetencourt, C. Bertarelli, G. Lanzani, F. Benfenati, *Nat. Nanotechnol.* **2020**, *15*, 296–306.
[52] V. Gujrati, J. Prakash, J. Malekzadeh-Najafabadi, A. Stiel, U. Klemm, G. Mettenleiter, M. Aichler, A. Walch, V. Ntziachristos, *Nat. Commun.* **2019**, *10*, 1114.
[53] J. B. Grimm, L. D. Lavis, *Nat. Methods* **2022**, *19*, 149–158.
[54] H. Kobayashi, M. Ogawa, R. Alford, P. L. Choyke, Y. Urano, *Chem. Rev.* **2010**, *110*, 2620–2640.
[55] F. Brøndsted, Y. Fang, L. Li, X. Zhou, S. Grant, C. I. Stains, *Chem. Eur. J.* **2024**, *30*, e202303038.
[56] Z. Zhao, C. B. Swartchick, J. Chan, *Chem. Soc. Rev.* **2022**, DOI 10.1039/D0CS00771D.
[57] Y.-F. Ou, T.-B. Ren, L. Yuan, X.-B. Zhang, *Chem. Biomed. Imaging* **2023**, *1*, 220–233.
[58] S. M. Usama, F. Inagaki, H. Kobayashi, M. J. Schnermann, *J. Am. Chem. Soc.* **2021**, *143*, 5674–5679.
[59] T. Ashida, T. Suzuki, TW201840738A, **2018**.
[60] R. Tapia Hernandez, M. C. Lee, A. K. Yadav, J. Chan, *J. Am. Chem. Soc.* **2022**, *144*, 18101–18108.
[61] K. Gutsmiedl, C. T. Wirges, V. Ehmke, T. Carell, *Org. Lett.* **2009**, *11*, 2405–2408.
[62] S. M. Pauff, S. C. Miller, *Org. Lett.* **2011**, *13*, 6196–6199.
[63] A. Toutchkine, WO2009152024A1, **2009**.
[64] E. D. Cosco, I. Lim, E. M. Sletten, *ChemPhotoChem* **2021**, *5*, 727–734.
[65] K. Rurack, M. Spieles, *Anal. Chem.* **2011**, *83*, 1232–1242.
[66] D. Razansky, A. Buehler, V. Ntziachristos, *Nat. Protoc.* **2011**, *6*, 1121–1129.
[67] L. Gao, Y. Kraus, A. Stegner, T. Wein, C. Heise, L. von Brunn, E. Fajardo-Ruiz, J. Thorn-Seshold, O. Thorn-Seshold, *Org. Biomol. Chem.* **2022**, *20*, 7787–7794.
[68] S. Roberts, A. Strome, C. Choi, C. Andreou, S. Kossatz, C. Brand, T. Williams, M. Bradbury, M. F. Kircher, Y. K. Reshetnyak, J. Grimm, J. S. Lewis, T. Reiner, *Sci. Rep.* **2019**, *9*, 8550.
[69] K. Cardinell, N. Gupta, B. D. Koivisto, J. C. Kumaradas, X. Zhou, H. Irving, P. Luciani, Y. H. Yücel, *Photoacoustics* **2021**, *21*, 100239.
[70] R. Yin, F. Brøndsted, L. Li, J. L. McAfee, Y. Fang, J. S. Sykes, Y. He, S. Grant, J. He, C. I. Stains, *Chem. Eur. J.* **2024**, e202303331.
[71] B. Du, C. Qu, K. Qian, Y. Ren, Y. Li, X. Cui, S. He, Y. Wu, T. Ko, R. Liu, X. Li, Y. Li, Z. Cheng, *Adv. Opt. Mater.* **2020**, *8*, 1901471.
[72] M. Wranik, T. Weinert, C. Slavov, T. Masini, A. Furrer, N. Gaillard, D. Gioia, M. Ferrarotti, D. James, H. Glover, M. Carrillo, D. Kekilli, R. Stipp, P. Skopintsev, S. Brünle, T. Mühlethaler, J. Beale, D. Gashi, K. Nass, D. Ozerov, P. J. M. Johnson, C. Cirelli, C. Bacellar, M. Braun, M. Wang, F. Dworkowski, C. Milne, A. Cavalli, J. Wachtveitl, M. O. Steinmetz, J. Standfuss, *Nat. Commun.* **2023**, *14*, 903.
[73] M. L. Landsman, G. Kwant, G. A. Mook, W. G. Zijlstra, *J. Appl. Physiol.* **1976**, *40*, 575–583.
[74] T. Gokus, A. Hartschuh, H. Harutyunyan, M. Allegrini, F. Hennrich, M. Kappes, A. A. Green, M. C. Hersam, P. T. Araújo, A. Jorio, *Appl. Phys. Lett.* **2008**, *92*, 153116.
[75] S. Liu, X. Zhou, H. Zhang, H. Ou, J. W. Y. Lam, Y. Liu, L. Shi, D. Ding, B. Z. Tang, *J. Am. Chem. Soc.* **2019**, *141*, 5359–5368.

Manuscript received: March 22, 2024
Accepted manuscript online: May 28, 2024
Version of record online: July 15, 2024